

# Classical general relativity effects by magnetars with slow rotation and a magnetic dipole

Alexander Mora-Chaverri, Edwin Santiago-Leandro, Francisco Frutos-Alfaro

May 7, 2024

## Abstract

In this contribution, the classical tests of general relativity using the Gutsunaev-Manko metric with slow rotation are obtained. This metric represents the spacetime of an object endowed with mass, magnetic dipole moment and angular momentum. These tests are the deflection of light, time delay, precession of the periastron and gravitational redshift. We also provide numerical estimations for real magnetars and magnetar candidates from the McGill magnetar catalogue, and for the Sun in the cycles of low activity. Our results find that the magnetic dipole contribution to the deflection of light is significant when compared to the rotation contribution. The magnetic dipole contributions to the periastron precession and the time delay are 3 and 6 orders of magnitude lower than the rotation contribution respectively. For the gravitational redshift, the contribution is negligible within the approximation presented.

## 1 Introduction

Since the formulation of General Relativity at the beginning of 20th century, there has been a motivation to find different solutions to Einstein's equations taking into account more complex physical phenomena. This was further motivated by Kerr's findings regarding a solution for a rotating massive object ( $m, J = ma$ ) in 1963 [15]. A few years later, Bonnor derived an exact solution referring to a static massive source carrying a magnetic dipole moment ( $m, \mu$ ), but this solution does not reduce to the well-known Schwarzschild metric when the magnetic field is zero [4]. Martin and Pritchett found an approximate magnetic dipole solution to the Einstein-Maxwell equations (EME) [22].

In 1987, Gutsunaev-Manko (GM) found an exact solution that does reduce to the Schwarzschild metric when the magnetic field vanishes [13]. The metric describes an object endowed with mass and a magnetic dipole moment ( $M, \mu$ ). The solutions were obtained using the Ernst formalism for the Lewis-Weyl-Papapetrou metric and these are solutions of the EME [8, 9]. Recently, approximate solutions to the EME were found that contain more relativistic multipole moments to better describe compact objects [10, 11].

The GM metric with rotation can be an interesting model to describe compact objects. For this reason, we add a component  $g_{t\phi}$  from Kerr's solution to first order in the angular momentum  $J$  ( $J^2 \sim 0$ ) to include rotation to the GM metric. Using a Reduce program, the slowly rotating GM metric is verified to be a solution to the EME. Spacetimes with magnetic dipole moment are rarely used to simulate or calculate astrophysical phenomena because of their complex form. The classical tests of general relativity, namely light deflection, periastron precession, time delay and gravitational redshift are calculated in this contribution.

Previous studies have estimated the magnetic dipole contribution to light deflection using different formalisms, but these studies do not have estimates for the other classical tests. Furthermore, these studies do not consider the rotation of the object or the coupling between the magnetic field and the spacetime. For instance, one method found in the literature consists on utilizing geometric optics (eikonal equation, Gauss-Bonnet theorem) or an approximate spacetime with non-rotating dipole moment to study nonlinear electrodynamics effect on light deflection [2, 6, 16, 17]. We use the GM metric with a slow rotation to obtain expressions for all classical test and provide numerical estimates utilizing The McGill Magnetar Catalog [23]. All calculations were done using Reduce or Python programs and these codes are also available upon request.

This paper is organized as follows. The GM metric is described in the second section. The inclusion of slow rotation (first order) in the GM metric is also described in this section. The classical tests of general relativity are described in section three. These expressions are obtained in the equatorial plane of the GM metric. In section four, we obtain the magnetic field for local non-rotating observe formalims (LNRO) for the GM metric [11]. Section

4 also includes a way to relate the parameter  $\alpha$  to realistic objects (such as different magnetars and the sun in the cycles of lower activity) and provide tables with estimates of each of the classical tests for these celestial objects. Some conclusions are discussed in section five. Throughout this article, we will be utilizing the geometrized unit system ( $G = c = 1$ ) for all algebraic expressions. For the numerical quantities, the units will be specified.

## 2 GM Metric

The GM spacetime describes a static spacetime with massive magnetic dipole [13], and is a solution of the EME. This metric in prolate spheroidal coordinates is

$$ds^2 = -f dt^2 + \frac{k^2}{f}(x^2 - y^2)e^{2\gamma} \left( \frac{dx^2}{x^2 - 1} + \frac{dy^2}{1 - y^2} \right) + \frac{k^2}{f}(x^2 - 1)(1 - y^2)d\phi^2, \quad (1)$$

Where

$$\begin{aligned} f &= \left( \frac{x-1}{x+1} \right) \left[ \frac{[x^2 - y^2 + \alpha^2(x^2 - 1)]^2 + 4\alpha^2 x^2(1 - y^2)}{[x^2 - y^2 + \alpha^2(x-1)^2]^2 - 4\alpha^2 y^2(x^2 - 1)} \right]^2 \\ e^{2\gamma} &= \left( \frac{x^2 - 1}{x^2 - y^2} \right) \left[ \frac{([x^2 - y^2 + \alpha^2(x^2 - 1)]^2 + 4\alpha^2 x^2(1 - y^2))^4}{[(1 + \alpha^2)(x^2 - y^2)]^8} \right]^2, \end{aligned} \quad (2)$$

And  $k$  and  $\alpha$  are parameters related with the mass  $m$  and the magnetic dipole  $\mu$  of the object through

$$\begin{aligned} k &= m \frac{(1 + \alpha^2)}{(1 - 3\alpha^2)} \\ \mu &= \frac{8m^2\alpha^3}{(1 - 3\alpha^2)^2}. \end{aligned} \quad (3)$$

The only component of the four potential  $A_\mu$  is

$$A_\phi = \frac{4k\alpha^3}{(1 + \alpha^2)} \left[ \frac{(1 - y^2)[2(1 + \alpha^2)x^3 + (1 - 3\alpha^2)x^2 + y^2 + \alpha^2]}{[x^2 - y^2 + \alpha^2(x^2 - 1)]^2 + 4\alpha^2 x^2(1 - y^2)} \right]. \quad (4)$$

The GM metric components in spherical coordinates  $(r, \theta, \phi)$  are obtained by means of the following transformation

$$\begin{aligned} kx &= r - m, \\ y &= \cos \theta. \end{aligned} \quad (5)$$

The metric takes the form

$$ds^2 = -V dt^2 + X dr^2 + Y d\theta^2 + Z d\phi^2 + W dt d\phi \quad (6)$$

Where the metric potentials are

$$\begin{aligned} V &= f, \\ X &= \frac{\beta e^{2\gamma}}{\eta f}, \\ Y &= \eta X, \\ Z &= \frac{\eta}{f} \sin^2(\theta), \\ W &= 0, \\ A_\phi &= \frac{4m^2\alpha^3}{(1 - 3\alpha^2)} \frac{P}{M} \sin^2(\theta), \end{aligned} \quad (7)$$

With

$$\begin{aligned}
\eta &= (r-m)^2 - \frac{m^2(1+\alpha^2)^2}{(1-3\alpha^2)^2}, \\
\beta &= (r-m)^2 - \frac{m^2(1+\alpha^2)^2}{(1-3\alpha^2)^2} \cos^2 \theta, \\
e^{2\gamma} &= \frac{(1-3\alpha^2)^2 \eta M^4}{((1-3\alpha^2)^2 \beta)^9}, \\
f &= \left(1 - \frac{2m(1+\alpha^2)}{(1-3\alpha^2)r + 4m\alpha^2}\right) \frac{M^2}{N^2}, \\
P &= \left[(1-3\alpha^2)^3 (2r-m)(r-m)^2 + m^3(1+\alpha^2)^2 (\alpha^2 + \cos^2 \theta)\right], \\
M &= \left[(1-3\alpha^2)^2 \beta - \alpha m^2(1+\alpha^2)\right]^2 + 4\alpha^2 m^2 (1-3\alpha^2)^2 (r-m)^2 \sin^2 \theta, \\
N &= \left[\left((1-3\alpha^2)(r-m) - m\alpha^2\right)^2 + m^2(\alpha^2 - (1+\alpha^2)\cos^2 \theta)\right]^2 - 4m^2 \alpha^2 (1-3\alpha^2)^2 \eta \cos^2 \theta.
\end{aligned} \tag{8}$$

When testing these expressions to make sure they satisfy the EME, we found that there is a misprint in the function  $f$  in spherical coordinates in the original article [13]. The value of  $f$  in spherical coordinates that satisfies the EME is the one in eq. (8). To carry out the following calculations in the next section, we need the metric components in Taylor series:

$$\begin{aligned}
V &= 1 - 2\mathcal{U}, \\
W &= -2\frac{J}{r} \sin^2 \theta, \\
X &= 1 + 2\mathcal{U} + 4(1 + 2\alpha^2(1 + 5\alpha^2) \sin^2 \theta) \mathcal{U}^2, \\
Y &= r^2(1 - 8(1 + 5\alpha^2)\alpha^2 \mathcal{U}^2 \cos^2 \theta), \\
Z &= r^2(1 - 8(1 + 5\alpha^2)\alpha^2 \mathcal{U}^2) \sin^2 \theta, \\
A_\varphi &= 8\alpha^3 m \mathcal{U} \sin^2 \theta = (1 - 3\alpha^2)^2 \mu \mathcal{U} \sin^2 \theta,
\end{aligned} \tag{9}$$

Where  $\mathcal{U} = m/r$ , and  $J$  is the angular momentum. The magnetic dipole moment is given by

$$\mu = 8m^2 \alpha^3 + \mathcal{O}(m^6, \alpha^5). \tag{10}$$

The non-diagonal term  $W$  includes rotation. This modification fulfils the EME at first order in  $J$  ( $J^2 \sim 0$ ). For real compact objects, the value of the magnetic parameter is on the order of  $10^{-2}$ .

### 3 Classical tests of general relativity

In general relativity, there are many interesting effects that can be easily observed in the solar system or in other systems. Some of these effects are known as the classical tests of general relativity: periastron precession, light deflection, gravitational redshift and time delay. These are phenomena that could not be explained using Newton's law of universal gravitation. For a historical account see [1, 5, 20]. When estimating these classical tests, it is of great interest to consider as many physical properties of the object that generates the curvature of space-time (mass, rotation, magnetic field, etc.) as possible, in order to obtain a better estimate of the contribution of each of these properties in the tests. In the next section we obtain mathematical expressions for all the mentioned tests. An expression for the contribution of the magnetic field in terms of the magnetic parameter ( $\alpha$ ) is also found.

### 3.1 Geodesic equation

The Lagrangian per unit mass is given by the expression

$$\mathcal{L} = \frac{1}{2} g_{\lambda\mu} \dot{x}^\lambda \dot{x}^\mu = \frac{1}{2} \left( \frac{ds}{d\tau} \right)^2, \quad (11)$$

Where  $\dot{x}^\mu = \frac{dx^\mu}{d\tau}$  ( $x^\mu = (t, r, \theta, \varphi)$ ).

There are two conserved quantities because the Lagrangian does not depend on  $t$  or  $\phi$ . These conserved quantities are

$$\begin{aligned} \frac{\partial \mathcal{L}}{\partial \dot{t}} &= -V\dot{t} + W\dot{\varphi} = -E, \\ \frac{\partial \mathcal{L}}{\partial \dot{\varphi}} &= Z\dot{\varphi} + W\dot{t} = L_z, \end{aligned} \quad (12)$$

Where  $E$  and  $L_z$  are the energy and angular momentum per unit mass, respectively. From (12), we get

$$\begin{aligned} \dot{t} &= \frac{EZ + WL_z}{W^2 + VZ} \equiv T, \\ \dot{\varphi} &= \frac{VL_z - EW}{W^2 + VZ} \equiv \Phi. \end{aligned} \quad (13)$$

From Lagrangian density and (13), we have the expression

$$\left( \frac{ds}{d\tau} \right)^2 = -VT^2 + X \left( \frac{dr}{d\varphi} \right)^2 \Phi^2 + Y \left( \frac{d\theta}{d\varphi} \right)^2 \Phi^2 + Z\Phi^2 + 2WT\Phi. \quad (14)$$

Solving for  $dr/d\varphi$  from (14)

$$\left( \frac{dr}{d\varphi} \right)^2 = \frac{1}{X\Phi^2} \left( \left( \frac{ds}{d\tau} \right)^2 + VT^2 - Y \left( \frac{d\theta}{d\varphi} \right)^2 \Phi^2 - Z\Phi^2 - 2WT\Phi \right) \equiv G(r, \theta), \quad (15)$$

The analysis is made in the equatorial plane  $\theta = \pi/2$ , then

$$\left( \frac{dr}{d\varphi} \right)^2 = G\left(r, \frac{\pi}{2}\right) \equiv F(r) = \frac{1}{X\Phi^2} \left[ \left( \frac{ds}{d\tau} \right)^2 + VT^2 - Z\Phi^2 - 2WT\Phi \right]. \quad (16)$$

Using the change of variable  $u = 1/r$ , we obtain

$$\begin{aligned} \left( \frac{du}{d\varphi} \right)^2 &= u^4 F(u), \\ \frac{d^2 u}{d\varphi^2} &= 2u^3 F + \frac{1}{2} u^4 \frac{dF}{du}. \end{aligned} \quad (17)$$

We used Reduce to obtain approximate expressions for classical tests of general relativity by means of Taylor series expansions up to order  $\mathcal{O}(M^3, J^2, \alpha^5)$ .

### 3.2 Angle of the deflection of light

Since we are studying the photon trajectory, it follows that

$$\left( \frac{ds}{d\tau} \right)^2 = 0 \quad (18)$$

By doing a Taylor expansion of  $F(u)$  in (17), we have

$$\frac{d^2 u}{d\varphi^2} + u = 3mu^2 - 24 \left(\frac{1}{b}\right)^2 m^2 \alpha^2 u - 120 \left(\frac{1}{b}\right)^2 m^2 \alpha^4 u - 2 \left(\frac{1}{b}\right)^3 J - 8 \left(\frac{1}{b}\right)^3 Jmu + \mathcal{O}(m^3, J^2, \alpha^5), \quad (19)$$

Where  $b = L_z/E$  is the impact parameter.

The next step is to find an expression for  $b$  in terms of the other constants. Evaluating the equation (16) at the maximum value  $u_m$  [3]

$$\left(\frac{du}{d\varphi}\right)^2 = u_m^4 F(u_m) = 0, \quad (20)$$

Where  $u_m$  is the inverse of closest approach in the curved spacetime  $r_{min}$ , this quantity is illustrated in the Figure 1. By expanding  $u_m^4 F(u_m)$  and solving for  $1/b$ , the expression becomes

$$\frac{1}{b} = u_m + 12m^2 \alpha^2 u_m^3 + 60m^2 \alpha^4 u_m^3 + \mathcal{O}(m^3, J^2, \alpha^5). \quad (21)$$

To solve (19) a perturbative Ansatz [1, 3] is required

$$\begin{aligned} u = & u_0 \cos \varphi \\ & + m(u_0^2 u_{m1} + u_0 u_m u_{m2} + u_m^2 u_{m3}) \\ & + m^2(u_0^3 u_{mm1} + u_0^2 u_m u_{mm2} + u_0 u_m^2 u_{mm3} + u_m^3 u_{mm4}) \\ & + \alpha^2 m^2(u_0^3 u_{mm\alpha 21} + u_0^2 u_m u_{mm\alpha 22} + u_0 u_m^2 u_{mm\alpha 23} + u_m^3 u_{mm\alpha 24}) \\ & + \alpha^4 m^2(u_0^3 u_{mm\alpha 41} + u_0^2 u_m u_{mm\alpha 42} + u_0 u_m^2 u_{mm\alpha 43} + u_m^3 u_{mm\alpha 44}) \\ & + J(u_0^3 u_{J1} + u_0^2 u_m u_{J2} + u_0 u_m^2 u_{J3} + u_m^3 u_{J4}) \\ & + mJ(u_0^3 u_{MJ2} + u_0^2 u_m u_{MJ3} + u_0 u_m^3 u_{MJ4}), \end{aligned} \quad (22)$$

Where  $u_0$  is the inverse of the closest approach in the flat spacetime  $r_0$ , this quantity is illustrated in the Figure 1. The other terms are functions that depend on  $\varphi$ . By substituting  $u$  in the differential equation, one can obtain 23 separate differential equations, of which 17 have the trivial solution

$$y(\varphi) = A \sin \varphi + B \cos \varphi. \quad (23)$$

Because of this, the arbitrary constants will be taken as zero. The other 6 equations are given by:

$$\begin{aligned} -\frac{d^2 u_{m1}}{d\varphi^2} - u_{m1} + 3 \cos^2 \varphi &= 0, \\ -\frac{d^2 u_{mm1}}{d\varphi^2} - u_{mm1} + 6u_{m1} \cos \varphi &= 0, \\ -\frac{d^2 u_{mm\alpha 23}}{d\varphi^2} - u_{mm\alpha 23} - 24 \cos \varphi &= 0, \\ -\frac{d^2 u_{mm\alpha 43}}{d\varphi^2} - u_{mm\alpha 43} - 120 \cos \varphi &= 0, \\ -\frac{d^2 u_{J4}}{d\varphi^2} - u_{J4} - 2 &= 0, \\ -\frac{d^2 u_{MJ4}}{d\varphi^2} - u_{MJ4} + 6u_{J4} \cos \varphi - 8 \cos \varphi &= 0. \end{aligned} \quad (24)$$

The solutions of (24) are

$$\begin{aligned}
u_{m1} &= \frac{1}{2}[3 - \cos(2\varphi)], \\
u_{mm1} &= \frac{3}{16}[20\varphi \sin \varphi + \cos(3\varphi)], \\
u_{mm\alpha 23} &= -12\varphi \sin \varphi, \\
u_{mm\alpha 43} &= -60\varphi \sin \varphi, \\
u_{J4} &= -2, \\
u_{mJ4} &= -10\varphi \sin \varphi.
\end{aligned} \tag{25}$$

Thus  $u$  takes the form

$$\begin{aligned}
u &= u_0 \cos(\varphi) + \frac{mu_0^2}{2}[3 - \cos(2\varphi)] + \frac{3m^2u_0^3}{16}[20\varphi \sin \varphi + \cos(3\varphi)] - 12m^2u_0u_m^2\alpha^2(1 + 5\alpha^2)\varphi \sin \varphi \\
&\quad - 2Ju_m^3 - 10mJu_0u_m^3\varphi \sin \varphi
\end{aligned} \tag{26}$$

Evaluating  $\varphi = 0$  in  $u$ , solving for  $u_0$  (taking second order in  $u_0$ ) and expanding, the result is

$$u_0 = u_m - mu_m^2 + 2m^2u_m^3 + 2Ju_m^3 + \mathcal{O}(m^3, J^2, \alpha^5) \tag{27}$$

Now, we can substitute  $\varphi = \pi/2 + \delta$  in 26, see Figure 1. We expand  $u$  in  $\delta$  to obtain an expression from which to find the deflection angle. The result is

$$\begin{aligned}
u &= \frac{1}{8}(-240\alpha^4m^2\pi u_0u_m^2 - 48\alpha^2m^2\pi u_0u_m^2 - 40mJ\pi u_0u_m^3 - 16Ju_m^3 + 15m^2\pi u_0^3 + 16mu_0^2) \\
&\quad + \frac{1}{16}u_0(-960\alpha^4m^2u_m^2 - 192\alpha^2m^2u_m^2 - 160mJu_m^3 + 69m^2u_0^2 - 16)\delta + \mathcal{O}(\delta^2)
\end{aligned} \tag{28}$$

Now, it applies that if  $\delta \approx 0$ , then  $u \approx 0$ , therefore from (28), we solve for  $\delta$  after doing a Taylor expansion. The result is

$$\delta = 2mu_m + \left(\frac{15\pi}{8} - 2\right)m^2u_m^2 - 2Ju_m^2 - 6\pi m^2\alpha^2u_m^2 - 30\pi m^2\alpha^4u_m^2 + \mathcal{O}(m^3, J^2, \alpha^5). \tag{29}$$

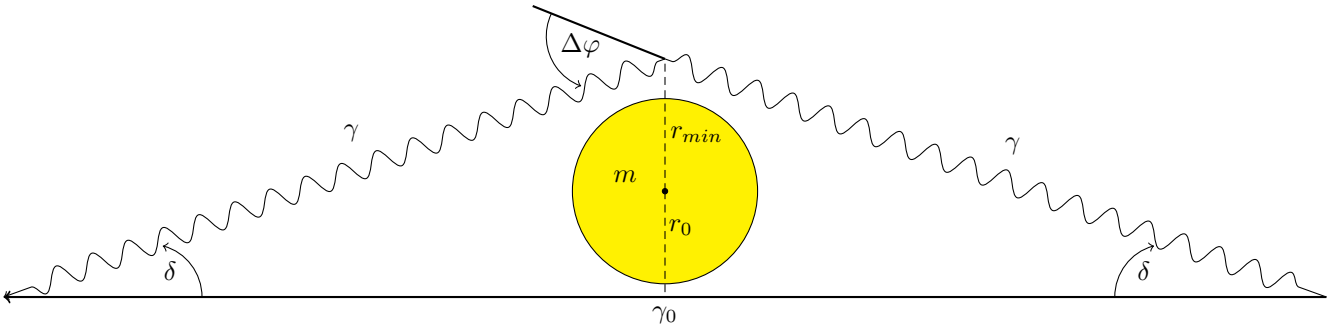


Figure 1: Deflection of light by object with mass  $m$ .

The total deflection angle is  $\Delta\varphi = 2\delta$

$$\Delta\varphi = 4mu_m + \left(\frac{15\pi}{4} - 4\right)m^2u_m^2 - 4Ju_m^2 - 12\pi m^2\alpha^2u_m^2 - 60\pi m^2\alpha^4u_m^2 + \mathcal{O}(m^3, J^2, \alpha^5) \tag{30}$$

The expression 30 contains the Schwarzschild correction up to second order[1, 3], the Kerr or Lense-Thirring correction up to first order [24, 27] and GM correction up to second order.

### 3.3 Periastron precession

In this case, the test particle is a massive, which means that

$$\left(\frac{ds}{d\tau}\right)^2 = -1 \quad (31)$$

By doing a Taylor expansion of  $F(u)$  in (17), we obtain

$$\begin{aligned} \frac{d^2u}{d\varphi^2} + u = & \left( \frac{2}{L_z^3} E(1 - E^2)J + \frac{m}{L_z^2} \right) \\ & + \left( -\frac{8E^3}{L_z^3} mJ + \frac{24}{L_z^2} (-E^2 + 1)m^2\alpha^2 + \frac{120}{L_z^2} (-E^2 + 1)m^2\alpha^4 \right) u \\ & + \left( 3m - \frac{24E^3}{L_z^3} m^2J + \frac{144}{L_z^3} E(E^2 - 1)m^2J\alpha^2 + \frac{720}{L_z^3} E(E^2 - 1)m^2J\alpha^4 \right) u^2 \\ & + \mathcal{O}(m^3, J^2, \alpha^5) \end{aligned} \quad (32)$$

To solve this differential equation, it is better to propose a solution of the form [1]

$$u = \frac{1}{l}[1 + \omega(\varphi)], \quad (33)$$

This proposed solution, similar to elliptic orbits, is illustrated in the Figure 2, where  $l$  is the semi-latus rectum and  $\omega(\varphi)$  is a periodic function that satisfies  $\omega(\varphi) \ll 1$ . Replacing (33) in (32) and expanding in  $\omega$ , the equation becomes

$$\begin{aligned} \frac{1}{l} \frac{d^2\omega}{d\varphi^2} = & \frac{1}{L_z^3} \left[ \frac{1}{l} (-120\alpha^4 E^2 L_z m^2 + 120\alpha^4 L_z m^2 - 24\alpha^2 E^2 L_z m^2 + 24\alpha^2 L_z m^2) \right. \\ & - \frac{8}{l} E^3 mJ - 2E^3 J + 2EJ + \frac{3}{l^2} L_z^3 m - \frac{L_z^3}{l} + mL_z \\ & + \frac{1}{l} \left( -120\alpha^4 E^2 L_z m^2 + 120\alpha^4 L_z m^2 - 24\alpha^2 E^2 L_z m^2 + 24\alpha^2 L_z m^2 - 8E^3 mJ + 6L_z^3 m \frac{1}{l} - L_z^3 \right) \omega \Big] \\ & + \mathcal{O}(\omega^2). \end{aligned} \quad (34)$$

The semi-latus rectum satisfies the expression

$$\begin{aligned} & \frac{1}{l} (-120\alpha^4 E^2 L_z m^2 + 120\alpha^4 L_z m^2 - 24\alpha^2 E^2 L_z m^2 + 24\alpha^2 L_z m^2) \\ & - 8E^3 mJ \frac{1}{l} - 2E^3 J + 2EJ + 3L_z^3 m \frac{1}{l^2} - L_z^3 \frac{1}{l} + mL_z = 0 \end{aligned} \quad (35)$$

Thus, the equation reduces to

$$\frac{d^2\omega}{d\varphi^2} = \frac{1}{L_z^3} \left[ \frac{1}{l} (-120\alpha^4 E^2 L_z m^2 + 120\alpha^4 L_z m^2 - 24\alpha^2 E^2 L_z m^2 + 24\alpha^2 L_z m^2 - 8E^3 mJ + 6L_z^3 m \frac{1}{l} - L_z^3) \omega \right] \quad (36)$$

From here, it is clear that the solution takes the form

$$\omega(\varphi) = A \sin(\sqrt{\Omega}\varphi) + B \cos(\sqrt{\Omega}\varphi), \quad (37)$$

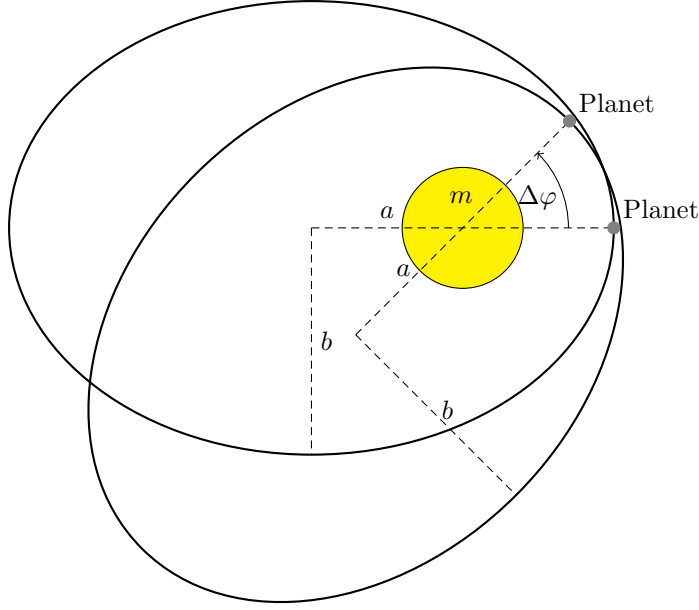


Figure 2: Periastron precession due to the curvature of spacetime.

Where

$$\Omega = \frac{1}{L_z^3} \left( -120\alpha^4 E^2 L_z m^2 + 120\alpha^4 L_z m^2 - 24\alpha^2 E^2 L_z m^2 + 24\alpha^2 L_z m^2 - 8E^3 m J + 6L_z^3 m \frac{1}{l} - L_z^3 \right) \quad (38)$$

A cycle is completed if

$$\varphi = \frac{2\pi}{\sqrt{\Omega}}. \quad (39)$$

The next step is to find a relation between the semi-latus rectum,  $E$  and  $L_z$ . This can be found with the post-newtonian relation, following the procedure shown in [26]

$$\begin{aligned} E = & 1 - \frac{m}{l} + \frac{L_z^2}{2l} - \frac{1}{2} \left( \frac{m}{l} \right)^2 - \frac{L_z^2}{2l^3} m - \frac{1}{2} \left( \frac{m}{l} \right)^3 \\ & - \frac{1}{8} \left( \frac{L_z}{l} \right)^4 - \frac{L_z^2 m^2}{4l^4} - \frac{5}{8} \left( \frac{m}{l} \right)^4 - 4\alpha^2 \left( \frac{m}{l} \right)^3 + \left( \frac{4m^2 L_z^2 \alpha^2}{l^4} \right) \\ & - 8\alpha^2 \left( \frac{m}{l} \right)^4 - 32\alpha^4 \left( \frac{m}{l} \right)^3 + 20 \left( \frac{L_z^2 \alpha^4 m^2}{l^4} \right) - 64 \left( \frac{\alpha m}{l} \right)^4 \\ & + \left( \frac{2L_z J}{l^3} \right) + \mathcal{O}(m^5, J^2, \alpha^5) \end{aligned} \quad (40)$$

In the previous expression, a higher order expansion in  $M$  was carried out to demonstrate the contribution of the magnetic field in the expression of  $E$ . For the magnitudes used in the calculations, only the massive contribution up to the second order is sufficient.

Using (40), (38) in (39), The angle after expanding becomes

$$\varphi = 2\pi + 6\pi \frac{m}{l} + 27\pi \frac{m^2}{l^2} - 8\pi \left( \frac{1}{L_z^3} + \frac{3}{2L_z l^2} \right) m J - 24\pi \frac{\alpha^2 m^2}{l^2} - 120\pi \frac{\alpha^4 m^2}{l^2} + \mathcal{O}(m^3, J^2, \alpha^5) \quad (41)$$

From which the periastron precession is found to be



$$\Delta\varphi = 6\pi\frac{m}{l} + 27\pi\frac{m^2}{l^2} - \frac{8\pi}{L_z^3}\left(1 + \frac{3L_z^2}{2l^2}\right)mJ - 24\pi\frac{\alpha^2 m^2}{l^2} - 120\pi\frac{\alpha^4 m^2}{l^2} + \mathcal{O}(m^3, J^2, \alpha^5) \quad (42)$$

The equation (42) contains Schwarzschild, Kerr and GM contributions and this result is in agreement with [1, 26].

### 3.4 Time delay

Let us take  $\theta = \pi/2$ , the first term of (26) and its derivative [7],

$$\begin{aligned} r \cos \varphi &= r_0, \\ \frac{dr}{d\varphi} \cos \varphi - r \sin \varphi &= 0, \\ \frac{d\varphi}{dr} &= \cot \varphi = \frac{r_0}{r\sqrt{r^2 - r_0^2}}. \end{aligned} \quad (43)$$

The quantities in these trigonometric relations are represented in the Figure 3.

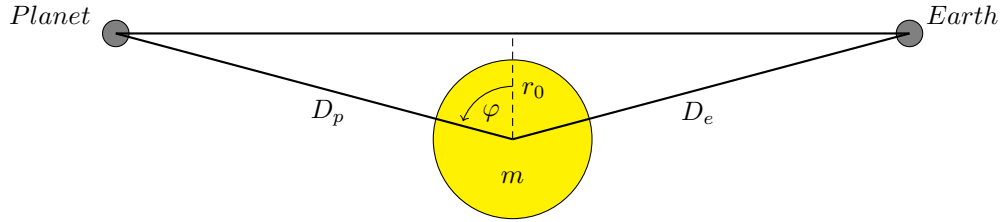


Figure 3: Representation of quantities in time delay.

Replacing (43) in the metric

$$ds^2 = -Vdt^2 + Xdr^2 + \frac{Zr_0^2}{r^2(r^2 - r_0^2)}dr^2 + \frac{2Wr_0}{r\sqrt{r^2 - r_0^2}}dtdr. \quad (44)$$

For electromagnetic waves, we have  $ds = 0$ , so that

$$0 = -V \left(\frac{dt}{dr}\right)^2 + X + \frac{Zr_0^2}{r^2(r^2 - r_0^2)} + \frac{2Wr_0}{r\sqrt{r^2 - r_0^2}} \left(\frac{dt}{dr}\right) \quad (45)$$

Solving (45) for  $dt/dr$ , taking the real solution and expanding, it is obtained

$$\begin{aligned} dt &= \frac{dr}{\sqrt{-r_0^2 + r^2}} \left( 2m + r - \frac{r_0^2 m}{r^2} - \frac{r_0^4 m^2}{2r^5} - \frac{2r_0^2 m^2}{r^3} + \frac{4m^2}{r} - \frac{2r_0 J}{r^2} - \frac{4r_0 m J}{r^3} \right. \\ &\quad \left. - \frac{8r_0^2 \alpha^2 m^2}{r^3} + \frac{4\alpha^4 m^2}{r} - \frac{40r_0^2 \alpha^2 m^2}{r^3} + \frac{20\alpha^4 m^2}{r} \right) + \mathcal{O}(m^3, J^2, \alpha^5) \end{aligned} \quad (46)$$

The equation (46) contains Schwarzschild, Kerr and GM contributions [1, 7]. Integrating this expression, we find that

$$\begin{aligned} \Delta t &= l_e + l_p + \left( 2 \ln(\Gamma_4 \Gamma_5) - \Gamma_1 \right) M + \frac{1}{16} \left( 45 \frac{\Gamma_6}{r_0} - 19 \Gamma_2 - 2r_0^2 \Gamma_3 \right) M^2 \\ &\quad - 2 \frac{\Gamma_1}{r_0} J - 4 \Gamma_2 M^2 \alpha^2 - 20 \Gamma_2 M^2 \alpha^4 - 2 \left( \frac{\Gamma_2}{r_0} + \frac{\Gamma_6}{r_0^2} \right) M J \end{aligned} \quad (47)$$

The first two terms in (47) are the time travel in flat spacetime, thus the time delay is given by

$$\begin{aligned}\Delta t_d = & \left(2 \ln(\Gamma_4 \Gamma_5) - \Gamma_1\right) M + \frac{1}{16} \left(45 \frac{\Gamma_6}{r_0} - 19 \Gamma_2 - 2 r_0^2 \Gamma_3\right) M^2 \\ & - 2 \frac{\Gamma_1}{r_0} J - 4 \Gamma_2 M^2 \alpha^2 - 20 \Gamma_2 M^2 \alpha^4 - 2 \left(\frac{\Gamma_2}{r_0} + \frac{\Gamma_6}{r_0^2}\right) M J,\end{aligned}\quad (48)$$

Where

$$\begin{aligned}l_e &= \sqrt{D_e^2 - r_0^2}, \\ l_d &= \sqrt{D_p^2 - r_0^2}, \\ \Gamma_1 &= \frac{l_e D_p + l_p D_e}{D_e D_p}, \\ \Gamma_2 &= \frac{l_e D_p^2 + l_p D_e^2}{D_e^2 D_p^2}, \\ \Gamma_3 &= \frac{l_e D_p^4 + l_p D_e^4}{D_e^4 D_p^4}, \\ \Gamma_4 &= \frac{1}{r_0} (l_e + D_e), \\ \Gamma_5 &= \frac{1}{r_0} (l_p + D_p), \\ \Gamma_6 &= 2 \arctan(\Gamma_4) + 2 \arctan(\Gamma_5) - \pi.\end{aligned}\quad (49)$$

### 3.5 Gravitational redshift

To calculate the redshift factor, a comparison of the proper time is performed for observers located at two different distance values. In the equatorial plane,  $\theta = \pi/2$ . This quantity is given by [1, 7]

$$\frac{\lambda'}{\lambda} = \sqrt{\frac{V(r')}{V(r)}} \quad (50)$$

Using a Taylor expansion in  $\alpha$ ,  $M$ , and  $J$ , we obtain

$$\frac{\lambda'}{\lambda} \approx 1 - m \left( \frac{1}{r'} - \frac{1}{r} \right) - \frac{1}{2} m^2 \left( \frac{1}{r'} + \frac{2}{r'r} - \frac{3}{r} \right) + \mathcal{O}(m^3, J^2, \alpha^5) \quad (51)$$

The gravitational redshift for the GM metric is approximately the gravitational redshift of the Schwarzschild metric. For this reason, this test will be excluded in the next section.

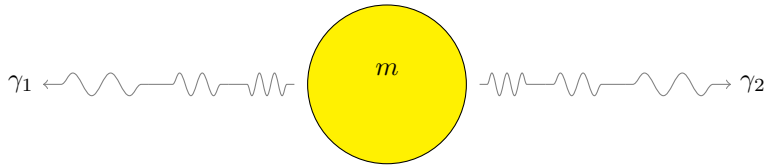


Figure 4: Gravitational redshift.

## 4 Numerical estimations

In this section, we describe the calculation for the magnetic field and the estimation for the magnetic parameter  $\alpha$  for different objects. With this information, one can then give numerical estimates for the different classical tests for realistic objects. Previous studies have given numerical estimations for the deflection angles using either the McGill Magnetar Catalog, or assuming a magnetar with superficial magnetic field of  $B_S = 10^{11}$  T [2, 16]. Both articles assume a mass of  $1.4 M_\odot$  and a radius of 10 km. Since it is difficult to know exactly the masses and radii of these systems, and how dependent these quantities are on the equation of state, we proceed to use the same values for mass and radius.

Regarding the rotation of the systems, it is also the case that, even if the periods of the systems are known, the exact angular momentum of these systems would also depend on the equation of state. With this in mind, we proceed to provide an upper bound for the angular momentum that is consistent with the slow rotation approximation. This will allow us to compare the magnetic dipole contribution to the classical tests with the rotation contribution without having to worry about whether a larger rotation would nullify the comparison. The smallest period of the McGill Magnetar Catalog is  $\sim 1.36$  s. So it is clear that, no matter what the mass distribution of a specific magnetar is, its angular momentum must be less than that of a spherical shell of the same mass. Thus,

$$J < \left(\frac{2}{3}mR^2\right) \left(\frac{2\pi}{T}\right) \quad (52)$$

Taking this into account, we take a spin parameter of  $J/m = 1 \text{ m}^1$ . Although it is common to associate NSs with highly rotating objects, it is important to note that magnetars tend to have much longer periods than normal radio pulsars [14]. The value of  $J/m$  chosen is significant enough to make a proper comparison between the rotation and magnetic dipole contributions to the classical tests, and is still small enough to be valid in the slow rotation approximation.

## 4.1 Magnetic field

It is important to mention that the main focus of this research is to analyze the contribution of the magnetic dipole when a careful treatment of the magnetic field and the curvature of spacetime it produces is taken into account. A more careful treatment of the magnetic field is important to make the estimations of the deflection angle and other tests of general relativity.

Even though these calculations are assuming a magnetic dipole, it is important to not only use the approximate equation of a magnetic dipole, but to consider how the magnetic field behaves in the metric under study. Following the work from [11], the electric and magnetic fields under a metric that has the form of equation (6) is

$$E_r = \frac{1}{\sqrt{X(VZ + W^2)}} \left[ \partial_r A_t - \frac{W}{\sqrt{Z}} \partial_r A_\varphi \right], \quad (53)$$

$$E_\theta = \frac{1}{\sqrt{Y(VZ + W^2)}} \left[ \partial_\theta A_t - \frac{W}{\sqrt{Z}} \partial_\theta A_\varphi \right], \quad (54)$$

$$H_r = \frac{1}{\sqrt{YZ}} \partial_\theta A_\varphi, \quad (55)$$

$$H_\theta = -\frac{1}{\sqrt{XZ}} \partial_r A_\varphi. \quad (56)$$

For the slow rotation and far field condition, we have

$$\frac{W}{\sqrt{Z}} \partial_r A_\varphi \approx 0, \quad (57)$$

$$\frac{W}{\sqrt{Z}} \partial_\theta A_\varphi \approx 0. \quad (58)$$

For this reason, the components of electromagnetic field are given by

$$E_r \approx 0, \quad (59)$$

$$E_\theta \approx 0, \quad (60)$$

$$H_r = \frac{1}{\sqrt{YZ}} \partial_\theta A_\varphi, \quad (61)$$

$$H_\theta = -\frac{1}{\sqrt{XZ}} \partial_r A_\varphi, \quad (62)$$

---

<sup>1</sup>For clarity, in SI units a  $c$  is added to the denominator, so that  $J/(mc) = 1 \text{ m}$ .

Where  $A_\varphi$  is given in equation (4). The approximate expression for the magnetic field is given by

$$\begin{aligned}
H_r &= 16\alpha^3 m^2 u^3 \cos \theta + 24\alpha^3 m^3 u^4 \cos \theta + 64\alpha^3 m^4 u^5 \cos^3 \theta \\
&\quad + 80\alpha^3 m^5 u^6 \cos(\theta)(3 \cos(\theta)^2 - 1) + \mathcal{O}(m^6, \alpha^5), \\
H_\theta &= 8\alpha^3 m^2 u^3 \sin \theta + 16\alpha^3 m^3 u^4 \sin \theta + 4\alpha^3 m^4 u^5 \sin \theta (12 \cos^2 \theta + 5) \\
&\quad + 16\alpha^3 m^5 u^6 \sin \theta (12 \cos^2 \theta + 1) + \mathcal{O}(m^6, \alpha^5).
\end{aligned} \tag{63}$$

The norm of magnetic field is given by

$$\begin{aligned}
H^2 &= g^{rr} H_r^2 + g^{\theta\theta} H_\theta^2 \\
&= \frac{1}{XYZ} \left[ \left( \partial_\theta A_\varphi \right)^2 + \left( \partial_r A_\varphi \right)^2 \right]
\end{aligned} \tag{64}$$

This allows us to obtain the magnetic field in any region of space. Because it is not easy to obtain analytically an expression for  $\alpha$  or  $\mu$  as a function of  $B$ , here we computationally obtain the value of  $\alpha$  that corresponds to a specific set of values  $(B_s, r, \theta)$  we are looking for. For  $B_s, r = 10 \text{ km}$  and  $\theta = \pi$  is utilized because the way that Olausen and Kaspi calculate the surface dipolar magnetic field strength of different magnetars in the McGill Magnetar Catalogue is measured specifically at the poles. [12, 18, 23].

Besides different magnetar candidates, having an estimation of the contribution of the magnetic dipole on the classical tests for the sun is also of interest. In this case, it is known that the magnetic field at the pole of the photosphere, in epochs of low activity, is around 10 G [21]. For this reason, the value of  $\alpha_\odot$  is obtained for  $(B_s, r, \theta) = (10^{-3} \text{ T}, 6.96 \times 10^8 \text{ m}, \pi)$ . For the angular momentum of the sun, the value of  $J = 1.88 \times 10^{41} \text{ kg m}^2 \text{ s}^{-1}$  is used from the calculation made by Rongquin et al. [25]. Once all the values are obtained, they are presented in different tables where the values are separated in the contributions from Schwarzschild, Kerr, and GM. This allows the reader to evaluate the contributions of the magnetic dipole on the classical tests of general relativity in relation to the contribution by the mass or the first order in rotation.

Table 1 contains the Schwarzschild to first and second order, and Kerr to first order contributions to the different classical tests. Since we are assuming the same masses, radii and angular momenta for all magnetars, these quantities do not change from one magnetar to the next, which is the reason there is a single value for each of the contributions. From now on, when we want to talk about the significance of the magnetic dipole moment in the classical tests, the values of Table 1 are the point of comparison.

Table 1: Numerical estimates for the Schwarzschild and first order Kerr contributions to the angle of light deflection, periastron precession and time delay for different magnetars and magnetar candidates of the McGill Magnetar Catalogue, taking  $m = 1.4 M_\odot$ ,  $J/m = 1 \text{ m}$  and  $r_{min} = r_0 = R = 10 \text{ km}$ . [23]

Quantity	Schw 1 <sup>st</sup> order	Schw 2 <sup>st</sup> order	Kerr 1 <sup>st</sup> order
$\Delta\varphi$ (as)	$1.7061 \times 10^5$	$6.8630 \times 10^4$	$1.7062 \times 10^1$
$\Delta\varphi$ (as/cent)	$6.0129 \times 10^1$	$1.0089 \times 10^{-5}$	$1.2044 \times 10^{-5}$
$\Delta t$ (s)	$9.6503 \times 10^{-4}$	$1.2603 \times 10^{-5}$	$3.6555 \times 10^{-9}$

Table 2 shows the deflection angle of light for different magnetars from the McGill Magnetar Catalogue [23]. The first column of the table corresponds to the name of the system, followed by the magnetic field, the value of  $\alpha$  that is equivalent to the specific magnetic field, then the total angle of deflection, and at the end the first and second order contributions of the magnetic dipole to the total angle of deflection. An interesting result from this analysis is that the contribution of the magnetic dipole moment is, on average, an order of magnitude larger than the first order term of a slow rotation. The amount of deflection related to the magnetic dipole moment is significant enough to be measurable if one takes into account that the angular resolution for the GAIA EDR3 is in the order of 0.5mas for objects of magnitude 20, which is comparable to the objects we are studying [19, 23]. For a magnetic field as high as the one from SGR 1806-20, the first order contribution of GM is actually 2 orders of magnitude larger than the first order contribution of rotation.

Table 2: Numerical estimates for the angle of light deflection for different magnetars and magnetar candidates of the McGill Magnetar Catalogue, taking  $m = 1.4 M_{\odot}$ ,  $J/m = 1$  m and  $r_{min} = R = 10$  km. [23]

Magnetar	Magnetic field $10^9$ (T)	$\alpha$ $10^{-2}$	$\Delta\varphi$ $10^5$ (as)	$\Delta\varphi_{GM1}$ $10^2$ (as)	$\Delta\varphi_{GM2}$ $10^{-2}$ (as)
CXOU J010043.1-721134	39.3	3.3204	2.3886	3.6660	202.09
4U 0142+61	13.4	2.3231	2.3905	1.7945	48.424
SGR 0418+5729	0.61	0.8305	2.3920	0.2293	0.7910
SGR 0501+4516	18.7	2.5952	2.3900	2.2394	75.411
SGR 0526-66	56.0	3.7336	2.3876	4.6351	323.05
1E 1048.1-5937	38.6	3.3007	2.3886	3.6226	197.33
1E 1547.0-5408	31.8	3.0953	2.3891	3.1858	152.61
PSR J1622-4950	27.4	2.9461	2.3894	2.8860	125.24
SGR 1627-41	22.5	2.7596	2.3897	2.5322	96.417
CXOU J164710.2-455216	6.59	1.8347	2.3911	1.1193	18.837
1RXS J170849.0-400910	46.8	3.5182	2.3881	4.1158	254.72
CXOU J171405.7-381031	50.1	3.5985	2.3879	4.3058	278.78
SGR J1745-2900	23.1	2.7838	2.3897	2.5768	99.846
SGR 1806-20	196	5.6419	2.3815	10.584	1684.6
XTE J1810-197	21.0	2.6971	2.3898	2.4188	87.974
Swift J1818.0-1607	35.4	3.2073	2.3888	3.4206	175.94
Swift J1822.3-1606	1.36	1.0848	2.3919	0.3913	2.3026
SGR 1833-0832	16.5	2.4895	2.3902	2.0607	63.856
Swift J1834.9-0846	14.2	2.3683	2.3904	1.8650	52.305
1E 1841-045	70.3	4.0252	2.3868	5.3875	436.45
3XMM J185246.6+003317	4.07	1.5628	2.3914	0.8121	9.9172
SGR 1900+14	70.0	4.0195	2.3868	5.3723	433.99
SGR 1935+2154	21.8	2.7308	2.3898	2.4796	92.453
1E 2259+586	5.88	1.7664	2.3912	1.0375	16.185
PSR J1846-0258 ##	4.88	1.6601	2.3913	0.9164	12.628

It is important to take into account that, even though it is unclear how big the exact angular momentum of these systems is, we made these calculations with an upper bound on  $J$ , which at the end was still a slow rotation. From the dependence between the magnetic field and the root of the period, one can conclude that it would make sense for a magnetar with very large magnetic field to have a comparatively slow rotation, which would make the magnetic dipole moment contribution on the deflection of light to be in the order of, if not larger, than the contribution of the slow rotation.

However, a more detailed analysis of the contribution of a highly rotating system to the metric would be necessary to compare the rotation and magnetic dipole moment contributions in more detail. Our results for the contribution of the magnetic dipole to the deflection of light differs from the one obtained by Kim, which is in the order of mas [16]. Even though the approach and the metric utilized varies, we believe the discrepancy is due to the different approach on the calculation of the magnetic dipole moment.

The results for the periastron precession and the time delay are presented in Tables 3 and 4 respectively. The way these tables are structured is very similar to the one explained for Table 2. The values for Table 3 were taken by estimating the precession of the periastron for a Mercury-like object orbiting the magnetar. With this in mind, the value for the semi-latus rectum is  $l = a(1 - e^2) \sim 0.37$  AU and the value for the specific angular momentum is  $L_z = a(1 - e)v_p \sim 2.74 \times 10^{15} \text{ m}^2 \text{ s}^{-1}$ , with  $v_p$  Mercury's periastron speed.

Notice that even in this extreme case for a magnetar, the contribution of the magnetic dipole moment to the precession of the periastron is, in the best of cases, 4 orders of magnitude smaller than the contribution for a slow rotation. It is clear that the periastron precession is more sensible to rotation than the magnetic dipole, compared to the light deflection angle.

Table 3: Numerical estimates for the precession of the periastron for different magnetars and magnetar candidates of the McGill Magnetar Catalogue, taking  $m = 1.4 M_{\odot}$ ,  $J/m = 1$  m and  $R = 10$  km. [23]

Magnetar	Magnetic field $10^9$ (T)	$\alpha$ $10^{-2}$	$\Delta\varphi$ $10^1$ (as/cent)	$\Delta\varphi_{GM1}$ $10^{-9}$ (as/cent)	$\Delta\varphi_{GM2}$ $10^{-13}$ (as/cent)
CXOU J010043.1-721134	39.3	3.3204	6.0129	9.8871	545.03
4U 0142+61	13.4	2.3231	6.0129	4.8398	130.60
SGR 0418+5729	0.61	0.8305	6.0129	0.6186	2.1332
SGR 0501+4516	18.7	2.5952	6.0129	6.0396	203.38
SGR 0526-66	56.0	3.7336	6.0129	12.501	871.26
1E 1048.1-5937	38.6	3.3007	6.0129	9.7700	532.20
1E 1547.0-5408	31.8	3.0953	6.0129	8.5918	411.58
PSR J1622-4950	27.4	2.9461	6.0129	7.7835	337.78
SGR 1627-41	22.5	2.7596	6.0129	6.8292	260.03
CXOU J164710.2-455216	6.59	1.8347	6.0129	3.0186	50.804
1RXS J170849.0-400910	46.8	3.5182	6.0129	11.100	686.97
CXOU J171405.7-381031	50.1	3.5985	6.0129	11.612	751.86
SGR J1745-2900	23.1	2.7838	6.0129	6.9496	269.28
SGR 1806-20	196	5.6419	6.0129	28.545	4543.2
XTE J1810-197	21.0	2.6971	6.0129	6.5234	237.26
Swift J1818.0-1607	35.4	3.2073	6.0129	9.2252	474.50
Swift J1822.3-1606	1.36	1.0848	6.0129	1.0554	6.2101
SGR 1833-0832	16.5	2.4895	6.0129	5.5577	172.22
Swift J1834.9-0846	14.2	2.3683	6.0129	5.0300	141.06
1E 1841-045	70.3	4.0252	6.0129	14.530	1177.1
3XMM J185246.6+003317	4.07	1.5628	6.0129	2.1902	26.746
SGR 1900+14	70.0	4.0195	6.0129	14.489	1170.4
SGR 1935+2154	21.8	2.7308	6.0129	6.6874	249.34
1E 2259+586	5.88	1.7664	6.0129	2.7981	43.651
PSR J1846-0258 ##	4.88	1.6601	6.0129	2.4715	34.058

A similar result is obtained from the values presented for the time delay in Table 4. In this case, the values of the time delay were estimated taking a light emitter a distance similar to Venus orbiting the magnetar and a receiver a distance similar to Earth orbiting the magnetar, this scenario was illustrated in the figure 3. In these conditions, the values for  $(D_e, D_p)$  are (1 AU, 0.72 AU). Similarly, here the best case scenario has a contribution of the magnetic dipole moment of 6 orders of magnitude less than the one produced by the slow rotation.

Table 5 shows the values obtained for the classical tests in the case of the Sun. It is important to emphasize that the magnetic dipole approximation for the photospheric magnetic field of the Sun is a good approximation only on the cycles of lower activity. Regarding the rotation of the Sun, the value for  $J_{\odot}$  mentioned previously would yield a spin parameter of  $J/m \sim 315$  m. If this surprises the reader, consider that the mass is distributed throughout  $6.96 \times 10^5$  km instead of 10 km, and the angular momentum is dependent on the square of the distance between the axis of rotation and the mass.

Here, it is less clear whether the slow rotation approximation would hold. Nevertheless, a similar result is found between the numerical estimations of our sun during low activity and the magnetars. For the deflection of light, the contribution of the magnetic dipole turns out to be of similar magnitude to the contribution from the slow rotation. However, both quantities are significantly smaller than the contribution from the mass. In the case of the periastron precession and the time delay, the contributions from the magnetic dipole moment turn out to be not measurable.

Table 4: Numerical estimates for the time delay for different magnetars and magnetar candidates of the McGill Magnetar Catalogue, taking  $m = 1.4 M_{\odot}$ ,  $J/m = 1$  m and  $r_0 = R = 10$  km. [23]

Magnetar	Magnetic field $10^9$ (T)	$\alpha$ $10^{-2}$	$\Delta t$ $10^{-4}$ (s)	$\Delta t_{GM1}$ $10^{-17}$ (s)	$\Delta t_{GM1}$ $10^{-20}$ (s)
CXOU J010043.1-721134	39.30	3.3204	9.7763	99.789	550.09
4U 0142+61	13.40	2.3231	9.7763	48.847	131.81
SGR 0418+5729	0.61	0.8305	9.7763	6.2430	2.1531
SGR 0501+4516	18.70	2.5952	9.7763	60.957	205.27
SGR 0526-66	56.00	3.7336	9.7763	126.17	879.36
1E 1048.1-5937	38.60	3.3007	9.7763	98.607	537.14
1E 1547.0-5408	31.80	3.0953	9.7763	86.717	415.41
PSR J1622-4950	27.40	2.9461	9.7763	78.558	340.92
SGR 1627-41	22.50	2.7596	9.7763	68.927	262.45
CXOU J164710.2-455216	6.59	1.8347	9.7763	30.466	51.276
1RXS J170849.0-400910	46.80	3.5182	9.7763	112.03	693.36
CXOU J171405.7-381031	50.10	3.5985	9.7763	117.20	758.84
SGR J1745-2900	23.10	2.7838	9.7763	70.142	271.78
SGR 1806-20	196.00	5.6419	9.7763	288.11	4585.4
XTE J1810-197	21.00	2.6971	9.7763	65.840	239.47
Swift J1818.0-1607	35.40	3.2073	9.7763	93.109	478.91
Swift J1822.3-1606	1.36	1.0848	9.7763	10.652	6.2678
SGR 1833-0832	16.50	2.4895	9.7763	56.093	173.82
Swift J1834.9-0846	14.20	2.3683	9.7763	50.767	142.37
1E 1841-045	70.30	4.0252	9.7763	146.65	1188.0
3XMM J185246.6+003317	4.07	1.5628	9.7763	22.106	26.995
SGR 1900+14	70.00	4.0195	9.7763	146.23	1181.3
SGR 1935+2154	21.80	2.7308	9.7763	67.495	251.66
1E 2259+586	5.88	1.7664	9.7763	28.241	44.057
PSR J1846-0258 ##	4.88	1.6601	9.7763	24.945	34.374

Table 5: Numerical estimates for the Schwarzschild, Kerr and GM contributions to the angle of light deflection, periastron precession and time delay for the Sun in epochs of low activity, taking  $\alpha = 9.0775 \times 10^{-2}$ ,  $m = M_{\odot}$ ,  $J = J_{\odot}$  and  $r_{min} = r_0 = R = R_{\odot}$ .

Quantity	Schw 1 <sup>st</sup> order	Schw 2 <sup>nd</sup> order	Kerr 1 <sup>st</sup> order	GM 1 <sup>st</sup> order	GM 2 <sup>nd</sup> order
$\Delta\varphi$ (as)	$1.7502 \times 10^0$	$7.2221 \times 10^{-6}$	$7.9409 \times 10^{-7}$	$2.8834 \times 10^{-7}$	$1.1880 \times 10^{-8}$
$\Delta\varphi$ (as/cent)	$4.2949 \times 10^1$	$5.1473 \times 10^{-6}$	$1.9412 \times 10^{-3}$	$3.7702 \times 10^{-8}$	$1.5534 \times 10^{-9}$
$\Delta t$ (s)	$9.0907 \times 10^{-4}$	$9.2210 \times 10^{-11}$	$8.9416 \times 10^{-12}$	$3.8052 \times 10^{-15}$	$1.5678 \times 10^{-16}$

## 5 Conclusions

In previous years, there has been an interest in studying in more detail the effect the magnetic dipole moment can have in the deflection of light for a system like a magnetar and in quantifying this effect. By employing the slow rotation GM metric, we have derived expressions that account for the mass, magnetic, and rotational effects. This has allowed us to obtain an estimation on the orders of magnitude of the contribution of all classical tests. Then, the McGill Magnetar Catalogue is used to estimate numerically the contribution of the magnetic dipole to the angle of light deflection, the periastron precession, and the time delay, and we have observed that the magnetic dipole effect can be quite comparable, and even greater than the rotational contribution depending on the analyzed test and physical conditions.

In the deflection of light results, it was found that the magnetic dipole contribution is significant, when compared to the rotational contribution. This is an important discovery, because a deflection of this magnitude might be an observable contribution in the future. For the periastron precession and the time delay, the contribution of the

magnetic dipole moment is present, but it is around 4 orders of magnitude less than the rotational contribution to first order for the periastron precession, and 8 orders of magnitude less for the time delay. In the case of the gravitational redshift, it was found that the magnetic dipole contribution to the gravitational redshift is negligible within the approximation presented. A more detailed study of the possible range of masses, radii and angular momenta, where the equations of state are taken into account, is important to continue with this research. The values were also calculated for the Sun in cycles of low activity, in which none of the classical tests yielded a significant magnetic dipole moment contribution.

## References

- [1] J. R. Arce-Gamboa, and F. Frutos-Alfaro, Classical General Relativity Effects to Second Order in Mass, Spin, and Quadrupole Moment, *Journal of Physics Communications*, 3(8):085018, 2019. <https://doi.org/10.1088/2399-6528/ab3b78>
- [2] N. Beissen, T. Yernazarov, M. Khassanov, S. Toktarbay, A. Taukenova, and A. Talkhat, Bending of Light by Magnetars within Generalized Born–Infeld Electrodynamics: Insights from the Gauss–Bonnet Theorem, *Symmetry*, 16(1):132, 2024. <https://doi.org/10.3390/sym16010132>
- [3] J. Bodenner, and C. M. Will, Deflection of light to second order: A tool for illustrating principles of general relativity, *American Journal of Physics*, 71 (8), 770–773, 2003. <http://dx.doi.org/10.1119/1.1570416>
- [4] W. B. Bonnor, An Exact Solution of the Einstein-Maxwell Equations Referring to a Magnetic Dipole, *Zeitschrift für Physik*, 190 (4), 444–445, 1966. <https://doi.org/10.1007/BF01327262>
- [5] C. Corda, The Secret of Planets’ Perihelion between Newton and Einstein, *Physics of the Dark Universe*, 32, 100834, 2021. <https://doi.org/10.1016/j.dark.2021.100834>
- [6] V. I. Denisov, I. P. Denisova, and S. I. Svertilov, Nonlinear Electrodynamic Effect of Ray Bending in the Magnetic-dipole Field, *Doklady Physics*, 46 (10), 705–707, 2001. <https://doi.org/10.1134/1.1415584>
- [7] R. D’Inverno, *Introducing Einstein’s Relativity*, Oxford University Press, Oxford, 1992.
- [8] F. J. Ernst, New Formulation of the Axially symmetric Gravitational Field Problem, *Physical Review*, 167 (5), 1175–1178, 1968. <https://doi.org/10.1103/PhysRev.167.1175>
- [9] F. J. Ernst, New Formulation of the Axially Symmetric Gravitational Field Problem. II, *Physical Review*, 168 (5), 1415–1417, 1968. <https://doi.org/10.1103/PhysRev.168.1415>
- [10] F. Frutos-Alfaro, Approximate Spacetime for Neutron Stars, *General Relativity and Gravitation* (2019), 51, 46, 2019. <https://doi.org/10.1007/s10714-019-2530-5>
- [11] F. Frutos-Alfaro, An Approximate Kerr-Newman-like Metric Endowed with a Magnetic Dipole and Mass Quadrupole, *ArXiv*, 2024. <https://doi.org/10.48550/arXiv.2308.00270>
- [12] J. E. Gunn and J. P. Ostriker, Magnetic Dipole Radiation from Pulsars, *Nature*, 221, 454–456, 1969. <https://doi.org/10.1038/221454a0>
- [13] Ts. I. Gutsunaev, and V. S. Manko, On the Gravitational Field of a Mass Possessing a Magnetic Dipole Moment, *Physics Letters A*, 123 (5), 215–216, 1987. [https://doi.org/10.1016/0375-9601\(87\)90063-6](https://doi.org/10.1016/0375-9601(87)90063-6)
- [14] J. A. Jawor, and T. M. Thauris, Modelling spin evolution of magnetars, *Monthly Notices of the Royal Astronomical Society*, 509 (1), 634–657, 2022. <https://doi.org/10.1093/mnras/stab2677>
- [15] R. P. Kerr, Gravitational Field of a Spinning Mass as an Example of Algebraically Special Metrics, *Physical Review Letters*, 11 (5), 237–238, 1963. <https://doi.org/10.1103/PhysRevLett.11.237>
- [16] J. Y. Kim, Deflection of Light by Magnetars in the Generalized Born–Infeld Electrodynamics, *The European Physical Journal C*, 82 (5), 485, 2022. <https://doi.org/10.1140/epjc/s10052-022-10435-5>



- [17] J. Y. Kim, and T. Lee, Light Bending by Nonlinear Electrodynamics under Strong Electric and Magnetic Field, *Journal of Cosmology and Astroparticle Physics*, 1111, 017–017, 2011.  
<https://doi.org/10.1088/1475-7516/2011/11/017>
- [18] V. Kim, A. Umirbayeva and Y. Airmuratov, Estimates of the Surface Magnetic Field Strength of Radio Pulsars, *Universe*, 9, 7, 2023. <https://doi.org/10.3390/universe9070334>
- [19] L. Lindegren et al., Gaia Early Data Release 3 - The astrometric solution, *Astronomy & Astrophysics*, 649 (A2), 2021. <https://doi.org/10.1051/0004-6361/202039709>
- [20] A. A. Ludl, Investigating Mono- and Quadrupole Gravitational Light Deflection by Jupiter, Lund Observatory, Lund University, 2011.  
<https://lup.lub.lu.se/luur/download?func=downloadFile&recordId=2158511&fileId=2158515>
- [21] D. H. Mackay, and A. R. Yeates, The Sun’s Global Photospheric and Coronal Magnetic Fields: Observations and Models, *Living Reviews in Solar Physics*, 9 (6), 2012. <https://doi.org/10.12942/lrsp-2012-6>
- [22] A. W. Martin, and P. L. Pritchett, Asymptotic Gravitational Field of the “Electron”, *Journal of Mathematical Physics*, 9 (4), 593–597, 1968. doi: <https://doi.org/10.1063/1.1664614>
- [23] S. A. Olausen, and V. M. Kaspi, The McGill Magnetar Catalog, *The Astrophysical Journal Supplement Series*, 212 (1), 6, 2014. <https://doi.org/10.1088/0067-0049/212/1/6>
- [24] A. Övgün, S. İzzet and J. Saavedra, Weak gravitational lensing by Kerr-MOG black hole and Gauss–Bonnet theorem, *Annals of Physics*, 411, 167978, 2019. <http://dx.doi.org/10.1016/j.aop.2019.167978>
- [25] C. Rongquin, The Angular Momentum of the Solar System, *Astronomy and Astrophysics* (Hans Publishers), 4 (2), 33–40, 2016. <https://doi.org/10.12677/AAS.2016.42004.org>
- [26] S. Subramaniam, On the Advance of Perihelia in the Kerr Spacetime, Master’s Thesis, ETH Zurich, 2018.  
<https://www.physik.uzh.ch/dam/jcr:81690208-6c06-45a1-8e3f-f319cb916f1c/report.pdf>
- [27] M. C. Werner, Gravitational lensing in the Kerr-Randers optical geometry, *General Relativity and Gravitation*, 44 (12), 3047–3057, 2012. <http://dx.doi.org/10.1007/s10714-012-1458-9>